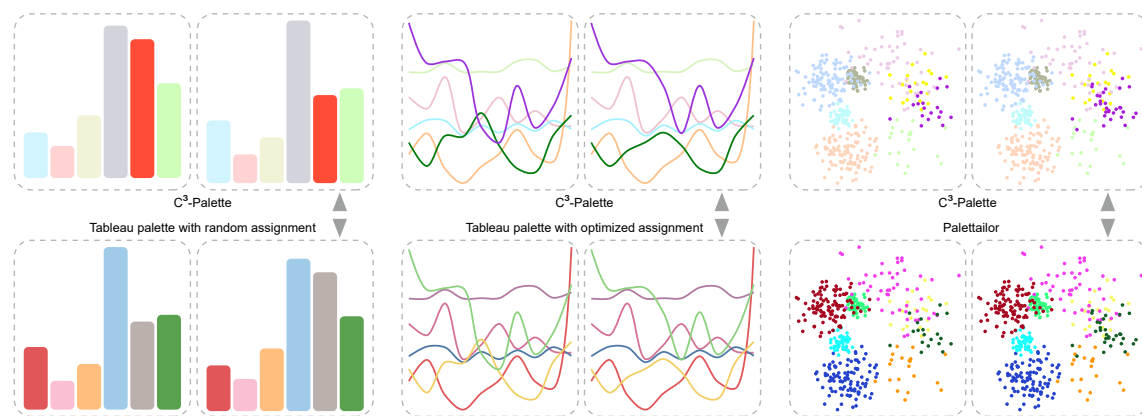


1 **C³-palette: Co-saliency based Colorization for Comparing Categorical
2 Visualizations**

3 ANONYMOUS AUTHOR(S)



22 Fig. 1. Results for different types of categorical data visualizations: (left) C³-palette versus Tableau palette with random assignment;
23 (center) C³-palette versus Tableau palette with optimal assignment; (right) C³-palette versus Palettaior [30]. Our co-saliency methods
24 (top) can highlight the changed classes while maintaining discrimination of classes.

25 Visual comparison within juxtaposed views is an essential part of interactive data analysis. In this paper, we propose a co-saliency
26 model to characterize the most co-salient features among juxtaposed labeled data visualizations while maintaining class discrimination
27 in the individual visualizations. Based on this model, we present a comparison-driven color design framework, enabling the automatic
28 generation of colors that maximizes co-saliency among juxtaposed visualizations for better identifying items with the largest magnitude
29 change between two data sets. We conducted two online controlled experiments to compare our colorizations of bar charts and
30 scatterplots with results produced by existing single view-based color design methods. We further present an interactive system and
31 conduct a case study to demonstrate the usefulness of our method for comparing juxtaposed line charts. The results show that our
32 approach is able to generate high quality color palettes in support of visual comparisons of juxtaposed categorical visualizations.
33
34

35 CCS Concepts: • Human-centered computing → Information visualization.

36 Additional Key Words and Phrases: Color Palette, Visual Comparison, Multi-Class, Juxtaposition

37 **ACM Reference Format:**

38 ANONYMOUS AUTHOR(S). 2018. C³-palette: Co-saliency based Colorization for Comparing Categorical Visualizations. In *Woodstock*
39 '18: ACM Symposium on Neural Gaze Detection, June 03–05, 2018, Woodstock, NY. ACM, New York, NY, USA, 21 pages. <https://doi.org/10.1145/1122445.1122456>

40 Permission to make digital or hard copies of all or part of this work for personal or classroom use is granted without fee provided that copies are not
41 made or distributed for profit or commercial advantage and that copies bear this notice and the full citation on the first page. Copyrights for components
42 of this work owned by others than ACM must be honored. Abstracting with credit is permitted. To copy otherwise, or republish, to post on servers or to
43 redistribute to lists, requires prior specific permission and/or a fee. Request permissions from permissions@acm.org.

44 © 2018 Association for Computing Machinery.

45 Manuscript submitted to ACM

53 1 INTRODUCTION

54
 Comparison is an indispensable task in data analysis and visualization. It often involves searching for categories (classes)
 55 with large or small changes among multiple categorical datasets. Comparison are usually achieved through juxtaposition
 56 of multiple categorical visualizations [13, 31] such as bar charts, line charts or multi-class scatterplots, where each
 57 category is commonly encoded by a unique color. While color codings are known to play an important role in helping
 58 viewers see differences between juxtaposed views [1, 13, 42], there is no color design scheme that optimizes visual
 59 comparisons, especially for the task of identifying the largest differences between charts [35].
 60

61
 A typical scenario would be a market analyst who uses comparisons to investigate the performance of a company
 62 across different countries over the last two years. S/he first would create a scatterplot for each year by showing the
 63 annual revenue and profit of each product by colorizing each point of the plot with a country label. After finding the
 64 two countries with the largest changes, s/he then examines the annual and monthly profits of various products in these
 65 countries with bar and line charts. Using the product name for color encoding, s/he is able to efficiently search the
 66 product with the largest differences from side-by-side shown bar and line charts.
 67

68
 The most common way to colorize juxtaposed views is to manually find a color mapping for a selected view while
 69 judging how well it fits to the other views. Such a trial and error procedure might converge to a desirable color
 70 mapping; however, the needed effort significantly increases with the numbers of classes and views. Although existing
 71 automated color selection approaches [6, 30, 43] allow to alleviate the effort for single view colorizations, the obtained
 72 color mapping might not be able to clearly reveal similarities or differences among multiple views. For example, the
 73 assignment of the Tableau palette for maximizing class separability (cf. [43]) in Fig. 1(center top) creates a visualization
 74 with better class discrimination, but the changed time series (see green and red curves in center bottom) are hard to
 75 identify. Although such classes of interest could be highlighted by fading out background classes using alpha blending,
 76 this inevitability would introduce visual ambiguities for overlapping classes [3] and potentially lead to a poor class
 77 separation. As far as we know, few existing visualization-oriented color selection tools (e.g., ColorBrewer [16] or
 78 Palettailor [30]) allow for colorizing multi-view visualizations, let alone supporting comparisons in juxtaposed views.
 79

80
 To fill this gap, we propose a comparison-driven color palette generation framework, which automatically generates
 81 appropriate color mappings for efficiently searching the largest differences from one categorical visualization to another.
 82 To achieve this goal, we propose a co-saliency model to characterize the most salient features among juxtaposed
 83 categorical visualizations that are likely to attract visual attention. We borrow the idea from the concept of image
 84 co-saliency [20], which was originally designed for summarizing salient differences between two similar natural images.
 85 Our co-saliency model allows to easily identify important features (e.g., changed classes) from juxtaposed categorical
 86 visualizations while maximizing the visual discrimination of classes in the individual visualizations. It is achieved by
 87 fusing two separate goals: class importance between visualizations and class contrast within them. Class contrast is
 88 based on perceptual separability between neighboring classes and with the background [43], while class importance is
 89 measured by summing up the changes of point positions and point numbers of each class, where the position change is
 90 quantified by using the Earth Mover's Distance (EMD) [37], a perceptual distance metric. Classes with large importance
 91 and small class separability (strong overlap with other classes) are more co-salient, while classes with small importance
 92 or large separability (more compact) are less co-salient.
 93

94
 By integrating our co-saliency model into existing categorical data colorization tools [30], we can automatically
 95 generate color mappings that maximize co-saliency among juxtaposed visualizations. The resulting color mapping
 96 schemes let classes with large importance pop out from the context and will attract viewers' attention, while at the same
 97 time maintaining the visual clarity of the overall visualization.
 98

time maximizing the perceptual separability between classes in the individual visualizations. By doing so, the major issue of a juxtaposition, that human have limited visual memory (see [41]), is greatly alleviated and visual searches can be performed with less cognitive costs [17]. The top of Fig. 1 shows the results generated by our colorization method, where the changed classes pop out and can easier be spotted than the ones in the bottom of Fig. 1. Our results are similar to the ones of alpha blending, but still maintain the separability between classes due to the different hues.

We evaluated our approach through carefully designed bar charts and scatterplots by comparing our colorized results with the ones produced by state-of-the-art palettes (e.g., Tableau [40] and Palettailor [30]). For bar charts, we replicated the experimental setting of Ondov et al. [35] but only performed the task of identifying a maximum difference from two horizontal juxtaposed bar charts. Next, we carried out studies with multi-class scatterplots generated by Lu et al. [30], whose counterparts were generated by changing the properties (point number and position) of several randomly selected classes. We first conducted a pilot study to verify the validity of our experimental setting and then ran two online studies: first, we investigated how well our generated palettes help users to identify changed classes of two scatterplots and second, we let them count class numbers in single scatterplots (discrimination task). Lastly, we conducted a case study to demonstrate how our system helps comparing juxtaposed visualizations with multiple line charts. The results show that our approach is able to produce color mappings optimized for supporting comparison and aligned with the state-of-the-art palettes in maximizing perceptual class separability.

A web-based color design tool, C³-palette¹, named by Co-saliency based Colorization for Comparing multi-class scatterplots, allows to show coordinated views and let users explore the relationship between multiple data sets with different color mapping schemes. The main contributions of this paper are as follows:

- We propose a multi-class data visualization co-saliency model for measuring the importance of each data item shown in juxtaposed visualizations and use this metric to automatically generate color mapping schemes for effective comparisons;
- We provide an interactive tool that demonstrates how our approach can be used for visually comparing categorical visualizations or highlighting important classes within single scatterplots; and
- We evaluate the effectiveness of the resulting color mapping schemes in supporting both, visual comparison and visual discriminability, with three online user studies and a case study (Section 4).

2 RELATED WORK

We divide previous works into those related to visual comparisons, color design for visualization, and visual saliency/co-saliency.

2.1 Visual Comparison

Visual comparison is an essential part of interactive data analysis, which is regarded as a high-level “compound task.” Gleicher et al. [14] provide a systematic review of techniques developed for supporting comparisons, three basic layout designs for comparative visualization are found: *juxtaposition*, *superposition* and *explicit encoding*. Among them, juxtaposition places different datasets in separate views without changes to the original visualization design due to its simplicity it is used in many applications [1, 29, 34]. However, such a design often creates cognitive burden because users need to maintain a mental image of one view for comparing it with another view [31]. Recently, Ondov et al. [35]

¹<https://c3-palette.github.io/>

and Jardine et al. [22] evaluated the perceptual effectiveness of different layouts for the comparison of bar charts with a few low-level tasks. They show that juxtaposition is less effective for tasks like finding “biggest delta between items”. Accordingly, Gleicher et al. [14] and L’Yi et al. [31] both suggested to carefully design visual encoding for improving their effectiveness. Therefore, our method facilitates visual comparison of categorical data by improving visual search using a pop-out effect [10] induced by our proposed color mapping scheme.

2.2 Color Design

For a complete review of color design techniques for visualization, we refer readers to surveys such as [42, 47]. We limit our discussion to techniques related to color design for categorical data visualization and specifically to the optimization of color mappings, color palette generation, and color design for multi-view visualization.

Color Mapping Optimization. Mapping each class to a proper color selected from a given palette is particularly helpful for categorical data visualization, since here no given order can be used. A few factors have been identified for guiding searches within such mappings. For example, Lin et al. [27] proposed to optimize the compatibility between class semantics and the assigned colors. Setlur and Stone [38] produced better results by using co-occurrence measures of color name frequencies. Kim et al. [23] incorporated color aesthetics and contrast into the optimization of color assignment for image segments. Recently, Wang et al. [43] proposed to maximize class discriminability based on color-based class separability, which takes into account spatial relationships between classes and the contrast with the background color. Once an assignment is done, the color of each class can be further optimized to better serve different purposes, such as reducing power consumption of displays [7], improving the accessibility of visualizations for visual impaired users [32], and a better class discrimination [26]. Almost all these methods aim to generate effective visualizations for single data sets, whereas our goal is to efficiently visualize salient class differences across multiple datasets with the same label information. One example are instances of the same dataset over time.

Color Palette Generation. To create an appropriate categorical color palette, the commonly used approach is to select one from a library of carefully designed palettes provided by online tools (e.g. ColorBrewer [16]). Colorgorical [15] further allows users to customize color palettes by generating them based on user-specified discriminability and preference importance. Recently, Palettailor [30] takes a further step by automatically generating categorical palettes for different types of charts, such as scatterplots, line and bar charts. However, all the aforementioned methods deal with single datasets, while our work focuses on visual comparisons within multiple datasets with some changed instances.

Multi-view Color Design. Multi-view visualizations are commonly used in multivariate analysis. Although a few design guidelines [44] have been proposed for constructing multi-view visualizations, few of them are related to color design. Qu et al. [36] recommended a set of color consistency constraints across views. Among them, is a high-level constraint that the same data field should always be encoded in the same way, which is related to our studied comparative visualization. Namely, all juxtaposed views should have the same color mapping scheme and a good scheme is able to help for seeing the differences between views. However, few works have been done for finding such schemes. The only exception is comparing multiple continuous scalar fields [42] with a global color map by merging overlapping value ranges in different datasets. Our work is the first to generate appropriate color mapping for comparing multiple categorical visualizations.

2.3 Visual Saliency & Co-saliency

Here we briefly review visual saliency models developed for visualizations and image co-saliency models.

Saliency for Visualization. The human visual system enables viewers to concentrate on salient regions of an image while ignoring others. This is guided by two major factors [8]: pre-attentive, bottom-up focus based on visual features (e.g., color, intensity and edges) and task-driven, top-down attention based on prior knowledge. Numerous saliency models [4] have been developed to mimic the bottom-up attention mechanism in computer vision. Most of them model image saliency as the contrast of image regions to their surroundings with low level features. Among them, the most influential one is the Itti model [19], which computes image saliency with differences surrounding a central region. Kim et al. [24] tailored this model to increase the visual saliency of selected regions within a volume dataset. JÄdnicke and Chen [21] employed Itti's model [19] to define a quality metric for evaluating visualizations. Recently, Matzen et al. [33] evaluated a variety of saliency models on a large dataset and explored why these models work poorly for visualizations. One major reason is that visualizations are often created for specific goals, whereas existing models are based on bottom-up attention. To overcome these weaknesses, they proposed a data visualization saliency (DVS) model by incorporating meaningful high-level features into Itti's model. However, this model is not designed on a class-level and cannot be directly used for categorical visualizations.

Image Co-Saliency. Unlike single image based saliency models, the co-saliency model estimates the saliency (importance) of each pixel within the context of related images. Jacobs et al. [20] developed a first co-saliency model for highlighting the most salient differences between two images. Later, this concept was extended for discovering common and salient objects/foregrounds from image collections [46]. Inspired by the original model [20], our work attempts to design an appropriate color mapping for visualizing the most co-salient features among juxtaposed labeled data visualizations. Following their findings that the co-salient features can be effectively characterized by fusing image changes and single image contrast, our co-saliency model relies on two factors: class contrast in the individual views and global features from in-between views (e.g., changes in the class structure).

3 CO-SALIENCY BASED COLOR DESIGN

Given N ($N \geq 2$) categorical visualizations with the same class labels (or a subset thereof), the j th visualization has M classes and n_j data items $\{\mathbf{x}_1^j, \dots, \mathbf{x}_{n_j}^j\}$, where each \mathbf{x}_t^j has a label $l(\mathbf{x}_t^j)$ and the i -th class (with n_i^j data points) consists of $\{\mathbf{x}_{i,1}^j, \dots, \mathbf{x}_{i,n_i^j}^j\}$, $i \in \{1, \dots, m\}$. For standard bar and line charts, M is equal to n_j but it is often smaller than n_j for scatterplots. All visualizations use the same background color \mathbf{c}_b and the same color mapping scheme $\tau : L \mapsto c$. Our goal is to find the best mapping τ that supports an effective comparison of multiple categorical visualizations.

In line with the design requirements for natural image comparison and categorial data visualization [13, 20, 30], our problem is formulated based on the following three design requirements:

- (i) **DR1:** highlighting the most concerned classes between visualizations as much as possible for an efficient comparison;
- (ii) **DR2:** maximizing the visual discrimination between classes in the individual visualizations for an efficient exploration of multi-class data; and
- (iii) **DR3:** providing flexible interactions for the exploration of relationships among the compared datasets.

Although visual comparison is an essential part of interactive data analysis, most of the existing colorization techniques [15, 30] attempt to meet DR2. The key challenge in meeting DR1 is that we need a proper model to characterize the most salient features in multiple visualizations. To address this issue, we propose our co-saliency model that calculates the saliency of each data item in the context of other similar visualizations. Integrating this model into the objective of a state-of-the-art color mapping generation framework [30], we can generate proper color mappings that

261 highlight salient differences between juxtaposed categorical visualizations while fostering a better visual discrimination
 262 of classes.
 263

264 265 266 3.1 Co-saliency for Multi-class Scatterplots

267 Following the definition of image co-saliency [20], we model class co-saliency with two factors: class importance
 268 between visualizations and class contrast within visualizations. The class importance describes how much each class
 269 should stand out from the visualization. Class contrast describes how much each class stands out from neighboring
 270 classes and the background, which is similar to perceptual class separability [2, 43]. Hence, we define two types of class
 271 contrasts: a local contrast with neighboring classes and a contrast with the background.
 272

273 Since point-based representations are very general in 2D visualization, we use two ($M = 2$) horizontally juxtaposed
 274 scatterplots to illustrate our method. Analogous to bottom-up image co-saliency models [11, 20], the co-saliency of the
 275 i th class is defined as the product between the class importance and class contrast scores to emphasize the target class
 276 and the co-saliency for M classes:
 277

$$278 E_{CoS} = \sum_i^M \left(\sum_j^N \frac{1}{n_i^j} \left(\lambda \alpha_i^j \exp(\theta_i) + (1 - \lambda) \beta_i^j f(\theta_i) \right) \right) \quad (1)$$

282 where θ_i is the importance of the i th class, n_i^j is the number of points of the i th class in the j th scatterplot, α_i^j is the
 283 local contrast with the neighboring classes of the i th class in the j th scatterplot, β_i^j is the contrast of the class to the
 284 background, and λ is the weight between them. The weight $1/n_i^j$ is used to alleviate class imbalances so that classes
 285 with small numbers of points and large changes can be highlighted.
 286

287 To better support DR1, we apply an exponential function to enlarge the weight of structural class changes, while
 288 using a piecewise function weighting the background contrast:
 289

$$290 291 292 f(\theta_i) = \begin{cases} \exp(\theta_i) & \text{if } \theta_i > \kappa \\ -\exp(\theta_i) & \text{else} \end{cases} \quad (2)$$

293 κ is a user-specified threshold with a default of zero. The reason for the two different weighting schemes is that classes
 294 with less or no changes might be treated as the background by viewers [46]. To suppress the saliency of such classes,
 295 we introduce a negative importance for them.
 296

297 **Local Contrast.** Given the j th scatterplot, we define the local class contrast based on the α -shape based point distinctness
 298 [30]. For each data point \mathbf{x}_t^j , we define its point distinctness as:
 299

$$300 301 302 \gamma(\mathbf{x}_t^j) = \frac{1}{|\Omega_t^j|} \sum_{\mathbf{x}_p^j \in \Omega_t^j} \frac{\Delta\epsilon(\tau(l(\mathbf{x}_t^j)), \tau(l(\mathbf{x}_p^j)))}{d(\mathbf{x}_t^j, \mathbf{x}_p^j)},$$

303 where Ω_t^j is set of k nearest neighbors of \mathbf{x}_t^j , $\tau(l(\mathbf{x}_p^j))$ is the color of \mathbf{x}_p^j , d is the Euclidean distance and $\Delta\epsilon$ is the CIELAB
 304 color distance. For the i th class, its local contrast is the sum of all points with the same class label in the scatterplot:
 305

$$306 307 308 \phi_i^j = \frac{1}{n_j} \sum_p^{n_j} \gamma(\mathbf{x}_p^j) \delta(l(\mathbf{x}_p^j), i) \quad (3)$$

309 where $\delta(l(\mathbf{x}_p^j), i)$ is one if the class label $l(\mathbf{x}_p^j)$ is i and else zero.
 310

313 If a class overlaps with different classes, the local contrast value will be high and the value will be small for a well
 314 separated class. Hence, the black class in the two scatterplots shown in Fig. 2(a) has a low contrast value (see Fig. 2(b))
 315 and the cyan class has a large value.
 316

317 **Background Contrast.** The contrast with the background is based on the so-called point non-separability $\rho(\mathbf{x}_t^j)$
 318 (rf. [43]), which is defined as the difference between two separation degrees:
 319

$$320 \quad \rho(\mathbf{x}_t^j) = b(\mathbf{x}_t^j) - a(\mathbf{x}_t^j). \quad (4)$$

322 where $b(\mathbf{x}_t^j)$ is the between-class separation degree and $a(\mathbf{x}_t^j)$ is the within-class separation degree. The measures are
 323 defined as weighted sums of color differences of \mathbf{x}_t^j with its neighborhood from the same and different classes:
 324

$$325 \quad a(\mathbf{x}_t^j) = \frac{1}{|\Omega_t^j|} \sum_{\mathbf{x}_p^j \in \Omega_t^j} \frac{\delta(l(\mathbf{x}_t^j), l(\mathbf{x}_p^j)) \Delta \epsilon(\tau(l(\mathbf{x}_t^j)), \mathbf{c}_b)}{d(\mathbf{x}_t^j, \mathbf{x}_p^j)}, \quad b(\mathbf{x}_t^j) = \frac{1}{|\Omega_t^j|} \sum_{\mathbf{x}_p^j \in \Omega_t^j} \frac{1 - \delta(l(\mathbf{x}_t^j), l(\mathbf{x}_p^j)) \Delta \epsilon(\tau(l(\mathbf{x}_t^j)), \mathbf{c}_b)}{d(\mathbf{x}_t^j, \mathbf{x}_p^j)}$$

328 When most neighbor points of \mathbf{x}_t^j have the same label as \mathbf{x}_t^j , $\rho(\mathbf{x}_t^j)$ is negative. However, such a negative $\rho(\mathbf{x}_t^j)$ makes
 329 the optimization in Eq. 1 meaningless, and the corresponding classes might be highlighted no matter how large the
 330 change of this class is. To address this issue, we use an exponential function to let $\rho(\mathbf{x}_t^j)$ always be positive while
 331 maintaining the monotonicity of the function. Accordingly, we define the contrast to the background of the i th class as:
 332

$$334 \quad \beta_i^j = \frac{1}{n_i^j} \sum_t^n \exp(\rho(\mathbf{x}_t^j)) \delta(l(\mathbf{x}_t^j), i). \quad (5)$$

337 As illustrated in Fig. 2(c), well-separated classes with large color differences from the background have large background
 338 contrast (blue and black classes), whereas the pink and cyan classes have relatively large background contrast values
 339 with a medium class separation.
 340

341 **Class Importance.** Class importance reflects whether a class should be highlighted or not. It can be specified by user
 342 or by some measures. In our paper, as a default we use the class change degree to represent the importance of each class.
 343 To quantify how users perceive structural changes of classes, we measure the difference between the class distributions
 344 in two scatterplots using the Earth Mover's Distance (EMD) [37], a perceptual metric. Suppose the i th class with two
 345 representations by two sets of points $\mathbf{X}_i^1 = \{\mathbf{x}_{i,1}^1, \dots, \mathbf{x}_{i,n_i^1}^1\}$ and $\mathbf{X}_i^2 = \{\mathbf{x}_{i,1}^2, \dots, \mathbf{x}_{i,n_i^2}^2\}$. Taking the Euclidian distance
 346 between points as the cost, we need to minimize the total matching cost
 347

$$349 \quad H(\mathbf{X}_i^1, \mathbf{X}_i^2) = \min_{\chi} \sum_t d(\mathbf{x}_{i,t}^1, \mathbf{x}_{i,\chi(t)}^2),$$

351 which constrains one-to-one mappings χ between points. This is the classic bipartite matching problem, which can
 352 be solved by the Hungarian method [25]. When the number of points of two sets is not equal, we further take the
 353 difference between the number of points into account. In doing so, the class change degree contains positional changes
 354 and changes of element numbers:
 355

$$357 \quad \theta_i = \frac{H(\mathbf{X}_i^1, \mathbf{X}_i^2)}{\min\{n_i^1, n_i^2\}} + v \frac{\|n_i^1 - n_i^2\|}{\max\{n_i^1, n_i^2\}} \quad (6)$$

360 both terms range within [0,1] and v is 1.0 as default value.
 361

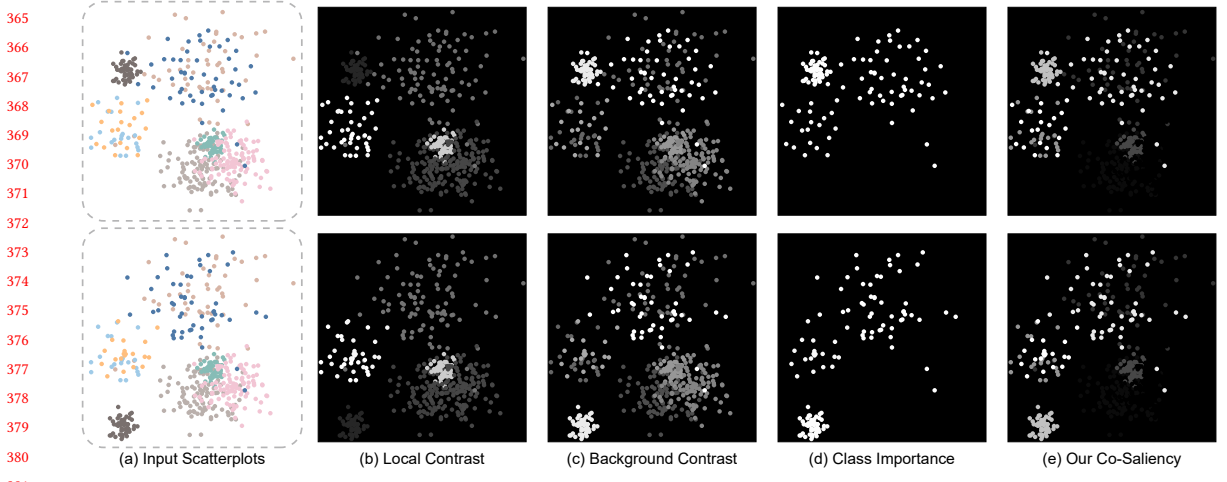


Fig. 2. Main components for computing co-saliency maps: For the two input scatterplots (a), our class-based co-saliency (e) is generated by fusing local contrast (b), background contrast (c), and class change degree (d). Brightness of points denotes value.

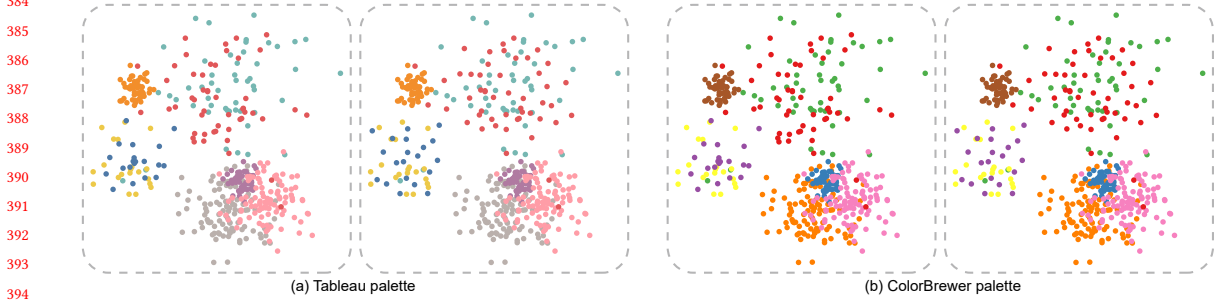


Fig. 3. Results generated by a co-saliency based color assignment with the existing Tableau-10 palette (a) and the ColorBrewer palette (b). Many existing palettes consist of bright colors only, where classes with smaller changes cannot be de-emphasized appropriately.

Fig. 2 shows an example of two 8-class scatterplots with three changing classes (orange, blue and black). Combining the class change degree with the two above-given contrast measures allows us to highlight salient differences and maintain the visual discrimination of the classes (see Fig. 2(e)).

3.2 Co-Saliency based Palette Generation

On the basis of our co-saliency model we meet DR1 and DR2 by a co-saliency based generation of color palettes. Taking the model in Eq. 1 as the objective within a state-of-the-art color assignment method [43], an optimal color mapping can be obtained from a given good palette. However, there are two major limitations **by not taking palette generation itself into account**: i) the model requires users to try many palettes for selecting a good one; and ii) the design of most existing palettes is not oriented towards visual comparison so that even the best color assignment cannot provide prominent cues for this task. Fig. 3 shows examples with the Tableau-10 palette and ColorBrewer palette [16]. Both results highlight several classes with minor changes (e.g., the bottom left purple class), and make it hard to identify the red class with the largest change even though it is very distinctive. Thus, we prompt users to use our co-saliency based palette generation method.

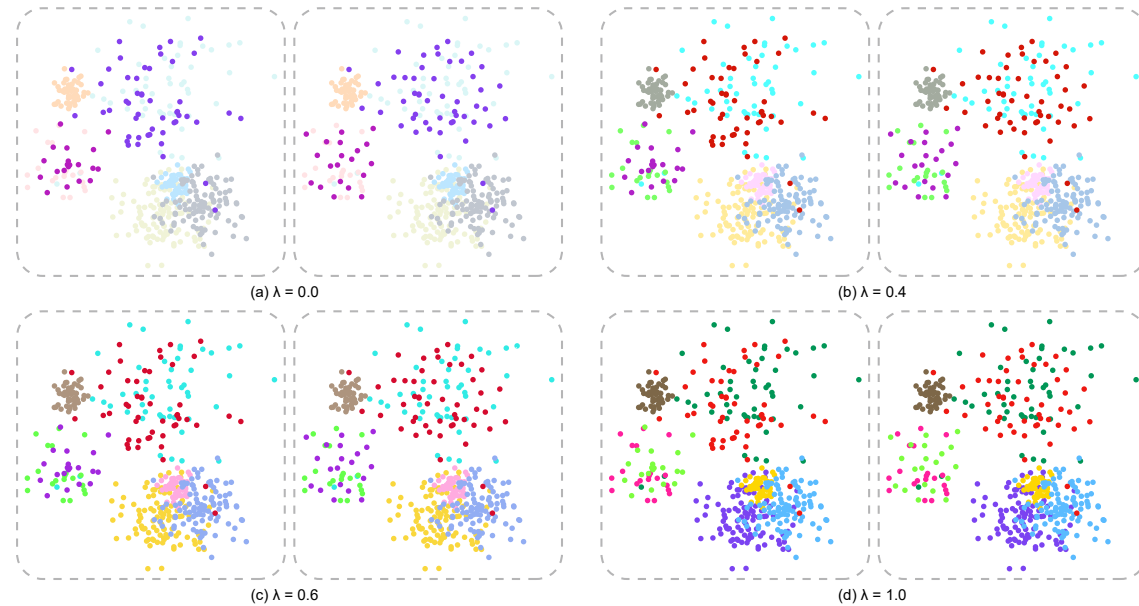
417 A recently proposed data-aware palette generation method by Lu et al. [30] automatically generates discriminable
 418 and preferable palettes by maximizing the combination of three palette quality measures: point distinctness, name
 419 difference, and color discrimination. By replacing the first measure with our co-saliency model, palette generation can
 420 be formulated as an optimization problem:
 421

$$\arg \max_{\tau} E(\tau) = \omega_0 E_{CoS} + \omega_1 E_{ND} + \omega_2 E_{CD}. \quad (7)$$

422 consisting of a co-saliency term E_{CoS} (see Eq. 1), a name difference term E_{ND} and a color discrimination term E_{CD} ,
 423 balanced by ω_0 , ω_1 and ω_2 . For more details about E_{ND} and E_{CD} , we refer readers to [30]. By using their optimization
 424 method, we are able to generate desired color palettes up to 40 colors in real time. For example, Fig. 4(b) shows an
 425 example which uses the same dataset as in Fig. 3, but improves the distinctness of the two changed classes while
 426 maintaining class separability.
 427

428 3.3 Parameter Effect

429 Besides using different weights for the terms in palette generation [30], our co-saliency model involves three parameters:
 430 the weight λ between the two contrasts, the threshold for the class importance κ , and v , which is related to the definition
 431 of the class change degree that is used as our default class importance. Since v is fixed in our experiments and the class
 432 importance can be specified by the user, we mainly discuss here the effects of λ and κ .
 433



460 Fig. 4. Effect of contrast weight λ : (a) result considering only contrast to the background; (b) result with $\lambda = 0.4$; (c) result with
 461 $\lambda = 0.6$; (d) result generated by only considering contrast with nearest classes.
 462

463 **Balancing Weight λ .** Although this parameter modulates the influence between class contrast with its neighbors and
 464 background, it offers a compromise between DR1 and DR2. As shown in Fig. 4(a), considering only the contrast to the
 465 background would result in a good 'pop out' effect, but other classes might be hard to discriminate. While considering
 466 only the contrast with nearest neighbors, such as done in Fig. 4(d), all the classes are easy to distinguish but the changed
 467 classes are no longer highlighted.
 468

469 classes are hard to find out. This is reasonable, because pre-attentive vision lets a bright and saturated color region
 470 within regions of de-saturated colors “pop-out” to the viewer [17]. In our experiments, we found that setting $\lambda = 0.4$ as
 471 a default value allows to simultaneously emphasize changes and preserve the discriminability between classes, see the
 472 example in Fig. 4(b).
 473

474 **Importance Threshold κ .** The importance threshold κ selects classes with large importance to be highlighted. With a
 475 default value of zero, all classes with an importance value larger than zero are ensured to be highlighted. Likewise, a
 476 large κ will de-emphasize classes with a small importance. We further allow users to specify κ by interaction through a
 477 widget in our interactive application.
 478

479 Note that our optimization inherently works for more than two categorical visualizations and the data with many
 480 classes. Since our contrast measures are built on the data-space nearest neighbour graphs, its produced palettes also
 481 work well for scatterplots with significant overlap between classes (see Fig.1 in the supplemental material).
 482

483 3.4 Bar and Line Charts

484 Like Palettailor [30], our color mapping generation method works also for other categorical visualization types such as
 485 bar or line charts. This is achieved by treating each bar or line segment in both views as a point and then using the
 486 same method to compute their class contrast. Taking line charts as an example, we order the line segments along the
 487 time axis and build a one-to-one mapping for line segments to compute θ_i . Doing so, lines with large changes will
 488 be highlighted while maintaining the discriminability between multiple lines in each chart. The same is done for bar
 489 charts, see Fig. 1. More results can be found in our supplementary material.
 490

491 4 EVALUATION

492 We evaluated the effectiveness of our method on supporting juxtaposed visual comparisons for different visualization
 493 types. This is achieved by comparing different colorized visualizations(i.e., bar charts and scatterplots) between our
 494 method and some existing methods. We conducted two online controlled experiments through Amazon Mechanical
 495 Turk (AMT) with 217 participants in total, each experiment contains different tasks for different visualization types:
 496

497 (i) Bar chart experiment:

- 500 • *Finding max delta task.* To evaluate how well our method can support people in *observing the largest change*
 501 for juxtaposed categorical bar charts;

502 (ii) Scatterplot experiment:

- 505 • *Spotting the difference task.* To evaluate how well our method can support people in *observing changes* for
 506 juxtaposed categorical scatterplots;
- 509 • *Counting class number task.* To evaluate whether our method can support the *visual separability* in each
 510 individual scatterplot, which is considered fundamental to juxtaposed comparison.

512 **Colorization Methods.** In each of our studies, we used six different ways to colorize datasets, including four benchmark
 513 methods (*Random Assignment*, *Optimized Assignment*, *Alpha Blending* and *Palettailor*) and two experimental methods
 514 based on our approach (*C³-Palette Assignment*, *C³-Palette Generation*):
 515

- 516 • *Random Assignment* is randomly selecting and assigning colors from Tableau-20 [40] palette to the classes.
 517 • *Optimized Assignment* uses the optimized assignment approach [43] for one of the two datasets with an input of
 518 Tableau-20 color palette.

- *Alpha Blending* is achieved by setting the opacity of each unchanged class to 0.5 while the changed classes remain to 1.0 based on *Optimized Assignment* result. We choose 0.5 since the results will be used in the discrimination task later.
- *Palettailor* uses the method proposed by Lu et.al [30] for palette generation. The palette is generated for one of the two datasets with the default settings.
- *C³-Palette Assignment* uses the color assignment optimization solution(Eq. 1) based on Tableau-20.
- *C³-Palette Generation* uses the unified color generation and assignment optimization method(Eq. 7), and produced the results with the default settings($\omega_0 = 1.0$, $\omega_1 = 1.0$, $\omega_2 = 1.0$ and $\kappa = 0$).

4.1 Experiment 1: Bar Chart Experiment

We test the performance of our method for bar charts through the *MAXDELTA* task which is used in Ondov et al.'s [35] comparison evaluation. Since the setup of this task is very similar to their work, we briefly describe the experimental design.

Task & Measure. *MAXDELTA task.* Following the methodology by Ondov et al. [35], we asked participants to find the bar that had the largest difference in the two charts. The titer value which is used to control the largest difference between the two bar charts, is recorded to measure the precision degree for people to make judgments about adjacent bar charts. Larger titer value indicates an easier trial. In addition to titer value(ranging from 0 to 1), we also recorded the answer, where a correct response recorded as 1 and wrong is 0.

Conditions & sample palette. Similar to the scatterplot experiment, we also tested the six conditions, including two experimental methods(*C³-Palette Assignment* and *C³-Palette Generation*), as well as four benchmark conditions(*Random Assignment*, *Optimized Assignment*, *Alpha Blending* and *Palettailor*). We used Tableau 20 palette for the assignment method due to its large range of brightness and saturation. Specifically, the original *Optimized Assignment* [43] did not apply their method to bar chart, we extended it by treating each bar as a point. *Alpha Blending* is based on the result of *Optimized Assignment* by changing the opacity of each class. Different to the scatterplot experiment, we run these methods in real-time since the bar charts are generated dynamically.

Bar chart generation. All the stimulus datasets used in this experiment are generated by the titer staircase method [35] in real time. Each pair of bar charts are generated differently depending on participant performance in the previous trial. For each condition method, the first trial generated bar charts with a titer of 0.5. An erroneous response made the titer of the next trial increase with +0.3(easier) while a correct answer lead to a decrease of -0.1(harder). To prevent participants from too many trials with low difficulty, we set 0.75 as the largest titer value. Each bar chart consists of 7 data points same as Ondov et al. [35].

Procedure. At the beginning of this task, we gave participants 4 training trials to make them familiar with our experiment. The first training trial is time-unconstrained which must be answered correctly while the time of other three trials are identical to the real test(1.5 seconds for impression) with the easiest(largest) titer value(0.75). We also inform participants how to do these trials. There were twenty trials for each condition methods(120 trials in total) and the order of the conditions are different between participants.

Results. We recruited 32 participants through the AMT, each participant went though all the six condition methods with random order. After the experiment, we run an accuracy-based outlier exclusion to filter participants whose overall proportion of correct trials was lower than two standard deviations from the mean of other workers. This procedure result in 2 participants be excluded from the results. Then we plotted the total error of all trials for each condition and the titrated signal with mean of final titers. As shown in Fig. 5(a), we can see that *C³-Palette Generation* has a significant

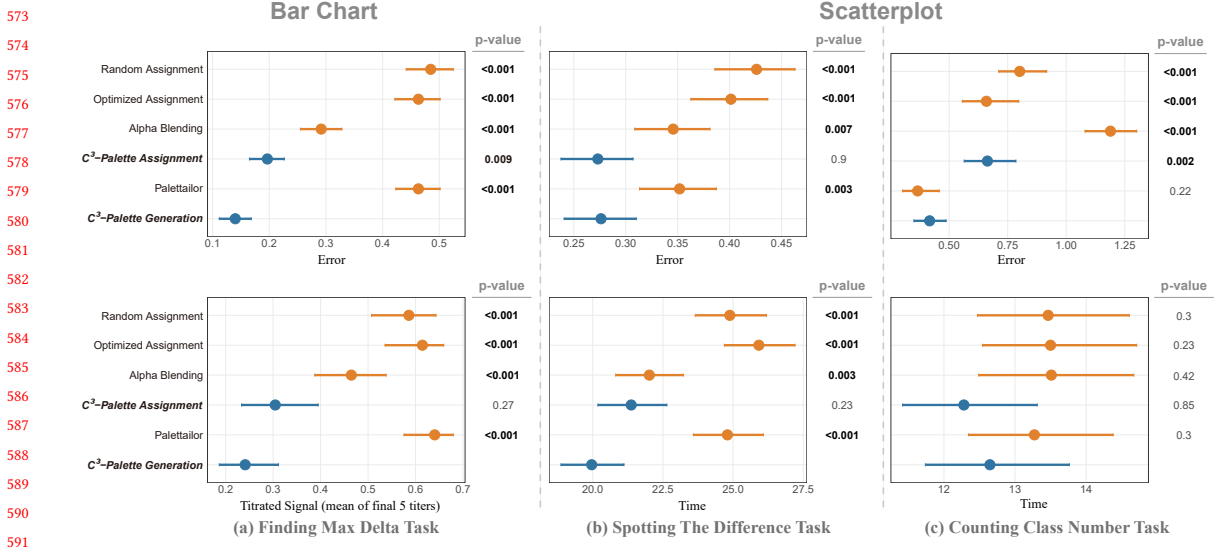


Fig. 5. Confidence interval plots and p-value from the Mann-Whitney test for the three online controlled experiments. Error bars represent 95% confidence intervals. Each p-value shows the statistical test result of *C³-Palette Generation* condition with other conditions. Smaller value means a better performance.

difference than other conditions in the error plot. For titrated signal, *C³-Palette Generation* has a better performance than existing methods while is comparable to *C³-Palette Assignment* with designer-crafted palette.

4.2 Experiment 2: Scatterplot Experiment

In addition to bar charts, we also conducted a scatterplot experiment to evaluate the effectiveness of our approach. Due to the complexity of the scatterplots, we adopted two tasks from the literature: *spotting the difference* and *counting class number*, each participant completed one of them.

Scatterplot Dataset Generation. The paired scatterplot datasets used in our studies were generated as follows. First, we designed a set of multi-class scatterplots, each containing 8 classes. Each class was generated using Gaussian random sampling and placed randomly in a 600×600 area. Similar to [30], these classes belong to one of the four settings of varying size and density: small & dense ($n = 50, \sigma = 20$), small & sparse ($n = 20, \sigma = 50$), large & dense ($n = 100, \sigma = 50$), and large & sparse ($(n = 50, \sigma = 100)$).

Then, for each scatterplot generated above, we produced its paired scatterplot by randomly choosing one or more classes and changing the positions or number of their data points. To systematically generate the changed classes, we defined *change magnitude*, which is related to three variables: *change type*, *change ratio* and *number of changed classes*. *Change type* defines how does the points change, contains change with *point number* and *point position*; *change ratio* defines how large the change of a type is, ranging from 0 to 1; and number of changed classes defines the number of classes that are changed, ranging from 1 to 3. We summarize our basic idea of data generation for each change type as below.

- *Point number:* For each class in the original scatterplot, we calculated the new point number by multiplying the original number by $(1 \pm \text{change ratio})$. The addition of points was implemented by generating them with the same

625 distribution as the original class. Subtraction was achieved by randomly deleting data points from the original
 626 class.

- 627 • *Point position*: Positional changes contain many types, such as changing the position of class centers and/or their
 628 shape. In our experiment, we use the two different positional changes that were mentioned above. For changing
 629 the center position of a class, we moved it into a certain *direction* with a specific *distance*. This was implemented
 630 by moving the center towards a random direction by a distance calculated by multiplying a maximal distance
 631 (400 by default) with the *change ratio*. For implementing shape changes, we defined the shape of a class as the
 632 bounding box of its data points. A shape change of a class was done by moving the density parameter of its
 633 Gaussian distribution into the opposite direction of the given value, i.e., a small & dense class ($n = 50, \sigma = 20$)
 634 would be changed into a small & sparse ($n = 50, \sigma = 50$) class. In order to produce a new shape for a class, we
 635 first calculated the one-to-one mapping between the newly-generated class and the original class using [25]
 636 and then linearly interpolated the position of a new point between the two corresponding points based on the
 637 *change ratio* parameter. We randomly choose one change type when disturbing the class to be changed.
 638

639 To simplify these independent variables, we produced 300 candidate scatterplot pairs for each change type, and then
 640 calculated the *change magnitude* for each pair using Eq. 6, and split all pairs into three levels: *small*, *medium*, and *large*.
 641 Next, without loss of fairness, we randomly selected 2 pairs from each change magnitude level for each change type
 642 and each number of changed classes. Thus in total we had 36 paired scatterplot in each of the two studies. The detailed
 643 dataset is showed in Table. 1.

644 Table 1. Grouping of Datasets: 36 datasets \times 6 conditions. C: condition; G: participant group; Position Small 1: point position change
 645 with small change magnitude for 1 changed class.

	C1	C2	C3	C4	C5	C6
Dataset 1: Position Small 1	G1	G2	G3	G4	G5	G6
Dataset 2: Position Small 1	G6	G1	G2	G3	G4	G5
Dataset 3: Position Small 2	G5	G6	G1	G2	G3	G4
Dataset 4: Position Small 2	G4	G5	G6	G1	G2	G3
Dataset 5: Position Small 3	G3	G4	G5	G6	G1	G2
Dataset 6: Position Small 3	G2	G3	G4	G5	G6	G1
Dataset 7: Position Medium 1	G1	G2	G3	G4	G5	G6
Dataset 8: Position Medium 1	G6	G1	G2	G3	G4	G5
...						
Dataset 35: Number Large 3	G3	G4	G5	G6	G1	G2
Dataset 36: Number Large 3	G2	G3	G4	G5	G6	G1

664 **Experiment Organization.** We tested the effects of the 6 method conditions across 36 paired multi-class scatterplot
 665 datasets using a *between-subject* experiment design. To avoid ordering effects, where the participant would get familiar
 666 with a dataset after seeing it several times, each participant was assigned to a group and saw a specific subset of datasets
 667 under different conditions. We used a Latin Square grouping (see Table. 1) to organize the trials for each participant.
 668

669 In addition, during the *spotting the difference* task, some participants might apply a “shortcut” strategy when seeing a
 670 class that is obviously more salient than the others, especially under the *C³-Palette Assignment* and *C³-Palette Generation*
 671 conditions. And for *spotting the difference* task, some participants might simply select 8 for all trials since they find
 672 many simple trials are 8 classes. Thus, for quality control, we added 4 sentinels which were very simple trials with 6
 673 classes, including only one changed class with a large change magnitude, and we assigned a de-saturated color to the
 674 classes, including only one changed class with a large change magnitude, and we assigned a de-saturated color to the
 675

677 changed class that made it less salient. All the classes are well separated. We add these 4 distractor trials to each group
678 to identify whether the participant is doing the task seriously and reject the results with more than two wrong trials.
679

680 Finally, there were 6 participant groups and each of them had 40 trials in total. To further avoid learning effects
681 between trials, we randomly shuffled the display orders of all scatterplot pairs, and randomly placed the two scatterplots
682 in each pair on the left or right side.
683

684 4.2.1 *Spotting the difference task.*

685 To evaluate how well our approach enables viewers observing changes between juxtaposed categorical scatterplots, we
686 conduct an online “spot-the-difference” experiment through Amazon Mechanical Turk (AMT) with 136 participants.
687

688 **Hypotheses.** We hypothesized that our approach would generally be more effective than the benchmark methods on
689 the juxtaposed comparison tasks, and that this effect would vary based on *change magnitude*.
690

691 **H1.** Our color generation method (*C³-Palette Generation*) outperforms the benchmark conditions (*Random Assignment*,
692 *Optimized Assignment*, *Alpha Blending* and *Palettailor*) on the task performance.
693

694 **H2.** Our color assignment method (*C³-Palette Assignment*) using a color palette with a large range of brightness and
695 saturation (*Tableau-20*) outperforms the benchmark conditions (*Random Assignment*, *Optimized Assignment*,
696 *Alpha Blending* and *Palettailor*) on the task performance.
697

698 **H3.** There would be an interaction effect between colorization methods and *change magnitude*. Specifically, the
699 difference between the achievements of our methods (*C³-Palette Generation* and *C³-Palette Assignment*) and that
700 of the benchmark methods (*Random Assignment*, *Optimized Assignment*, *Alpha Blending* and *Palettailor*) would
701 vary based on *change magnitude*.
702

703 **Task & Measures.** In this experiment, each participant was asked to perform a *spot-the-difference* task. Inspired by the
704 “Spot the Difference” game where one needs to compare a pair of similar pictures to detect their differences [12], we
705 asked participants to identify all the classes that have been changed between two scatterplots. At the beginning of
706 each trial, the number of changed classes was provided. Each participant was asked to select all the changed classes by
707 clicking the points belonging to these classes in either of the scatterplots.
708

709 For each participant, we measured the *time* taken for each trial, and counted the errors (0/1) indicating whether
710 the actual changed classes are aligned with the participant’s response. Note that if any of the changed classes was
711 mistakenly identified, the trial would be considered as “wrong” (1).
712

713 While the participant was instructed to do the task “*as accurately as possible*”, we set a 60-second time limit for each
714 trial for fear that user might spend too much time on the trial. If the participant could not find all the changed classes
715 during the time limit, they were directed to the next trial. This was done since we observed from the pilot study that
716 when participants spent too much time on a single trial, they may decide to quit by selecting a class randomly (which
717 would lead to an incorrect answer) or to spend more time till they get the correct answer (which would lead to an
718 increasing time spent on the trials). Such subject decisions would add noise to our measurements. Thus we added a
719 60-second time limit, which was indicated by our pilot study: over 92% of the trials were completed within that time.
720

721 **Pilot Study & Power Analysis.** We conducted a pilot study involving 28 participants to check the experimental setup
722 and determine the parameters, such as the time limit for a trial. Harnessing by the pilot study, we also obtained our
723 expected effect sizes, which were in further fed into a power analysis. With an effect size Cohen’s *d* of 0.4, alpha level of
724

Table 2. Participants details for each task of the scatterplot experiment.

Task & Group	Spotting the Difference		Counting class number	
	Pilot(28)	Formal(108)	Pilot(29)	formal(52)
Group 1	5	18	5	9
Group 2	5	17	5	8
Group 3	5	19	4	8
Group 4	3	17	5	9
Group 5	5	19	5	9
Group 6	5	18	5	9

0.05 and beta level of 0.8, the power analysis suggested a minimum number of 100 participants for the spot-the-difference task. See Fig.3(a) in the supplementary material for more details.

Participants. We recruited 108 participants(as shown in Table. 2) for the experiment on Amazon Mechanical Turk. According to the completion time in the pilot study, we paid each participant \$1.5 for the task based on the US minimum hourly wage. No participant claimed color vision deficiency on their informed consent.

Procedure. Each participant went through the following steps in our experiment: (i) viewing a user guide of the task and completing three training trials; (ii) completing each trial as accurately as possible; (iii) providing demographic information.

4.2.2 Results.

Following previous studies, we analyzed the results using 95% confidence intervals, and also conducted Mann-Whitney tests to compare the differences between conditions. The non-parametric test was used due to observations of non-normally distributed data from our pilot study. In addition, we computed the effect size using *Cohen's d*, i.e., the difference in means of the conditions divided by the pooled standard deviation. We used ANOVA to examine the interaction effect between variables.

Results of the online experiment are shown in Fig.5 (b). First, we found that our approach (*C³-Palette Assignment* and *C³-Palette Generation*) leads to a significantly lower error rate than all benchmark conditions. For the completion time, *C³-Palette Generation* has significantly less time ($p = 0.003$) than *Alpha Blending* condition while *C³-Palette Assignment* has no significant difference ($p = 0.095$), and our approach has significantly less time than all other benchmark conditions($p < 0.001$). The result indicates that our palette generation method (*C³-Palette Generation*) has a better performance than benchmark conditions in the “spot-the-difference” task (**H1** confirmed). As for color palettes with a larger range of brightness and saturation, our approach (*C³-Palette Assignment*) is better than most conditions and is at least comparable to the *Alpha Blending* condition (**H2** confirmed).

Finally, we did not find significant interaction effect between *colorization methods* and *change magnitude*, meaning that the effect of our method is not necessarily influenced by the magnitude of change between the two scatterplots (**H3** not confirmed).

4.2.3 Counting class number task.

To evaluate whether our approach can fundamentally support the visual separability of the classes in each scatterplot, we conducted an online “counting class number” experiment through AMT with 81 participants. The experimental design was similar to the first study, but we set up with different task during the experiment. We expected to see

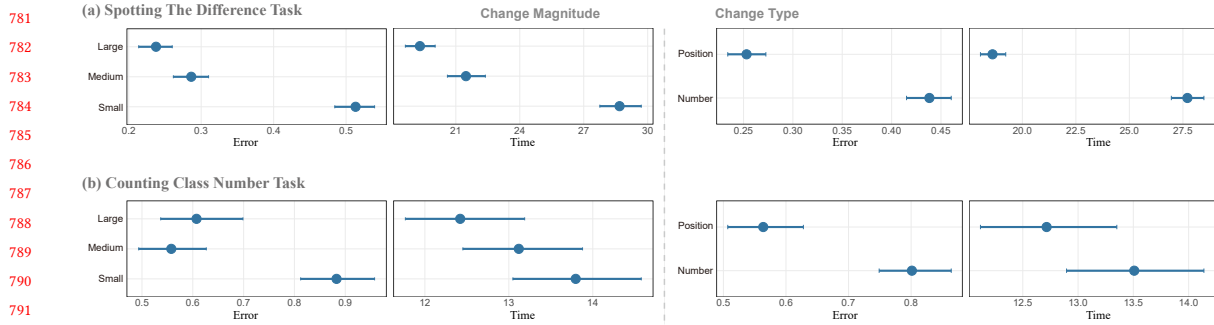


Fig. 6. Confidence interval plots for the two online controlled experiments. (left) Plots for *change magnitude* based on error and time; (right) plots for *change type* based on error and time. [This might be moved to supplemental material.]

different patterns of the discriminability across different conditions. Specifically, our methods would lead to a shorter error and time than *Random Assignment* and *Alpha Blending* conditions.

Hypotheses. We hypothesized that our approach would generally be more effective than the benchmark methods on the discrimination tasks, and that this effect would not vary based on *change magnitude*.

H1. Our color generation method (*C³-Palette Generation*) outperforms the benchmark conditions (*Random Assignment*, *Optimized Assignment*, *Alpha Blending*) and our assignment method(*C³-Palette Assignment*), while is comparable to *Palettailor* on the task performance.

H2. Our color assignment method (*C³-Palette Assignment*) based on *Tableau-20* outperforms the benchmark conditions (*Random Assignment*, *Alpha Blending*), while is comparable to *Optimized Assignment* condition on the task performance.

H3. There would be no interaction effect between colorization methods and *change magnitude*.

Task & Measures. Following previous methodologies [30, 43], each participant was asked to perform a *counting class number* task. We asked participants to identify how many classes(colors) are there in the given two scatterplots and then choose an answer among several options below the two scatterplots. We recorded the participant's answer and response time for each trial, and counted the *error* by calculating the differences between the participant's answer and the actual number of classes.

Pilot Study & Power Analysis. This setting is similar to the previous task. We invited 29 participants to do the pilot study and the results were in further fed into a power analysis. With an effect size Cohen's *d* of 0.6, the power analysis suggested a minimum number of 50 participants for the discriminability task. See Fig.3(b) in the supplementary material for more details.

Participants. We finally recruited 52 participants(as shown in Table. 2) for the experiment on Amazon Mechanical Turk. According to the completion time in the pilot study, we paid each participant \$1.5 for the task based on the US minimum hourly wage. No participant claimed color vision deficiency on their informed consent.

4.2.4 Results.

Results of this visual separability experiment are shown in Fig.5 (c). Through this study we first found that *C³-Palette Generation* is comparable to *Palettailor* while it leads to a significantly lower error rate($p \leq 0.001$) than all other

benchmark conditions. Specifically, *C³-Palette Generation* has a significantly lower error rate($p = 0.002$) than *C³-Palette Assignment*(H1 confirmed). Second, *C³-Palette Assignment* has higher performance than the benchmark conditions (*Random Assignment*, *Alpha Blending*) and is comparable to *Optimized Assignment*(H2 confirmed). There's no significant difference on completion time. Finally, we did not find a significant interaction effect between *colorization methods* and *change magnitude*, meaning that the effect of different methods for visual discriminability is not necessarily influenced by the magnitude of change between the two scatterplots(H3 confirmed).

4.3 Discussion

In summary, we evaluated the effectiveness of our approach against the benchmark conditions through three online studies, including one bar chart experiment, and two scatterplot experiment. We found that first, our methods outperform the benchmark methods on juxtaposed comparison tasks, and their effects are not necessarily influenced by the change magnitude of the two scatterplots. The performance of *Optimized Assignment* is comparable to *Random Assignment*, this is reasonable, since the *Optimized Assignment* mainly cares about the visual separability of different classes, thus it might assign the less salient color to the changed class while *Random Assignment* would assign salient color even though the whole separability of the scatterplot is not very good. This also provides an explanation for the bad performance of *Alpha Blending* which also assigns low contrast colors to changed classes. We show some examples for *Alpha Blending* in Figs.(1,2) in the supplementary material.

Second, our experimental methods (*C³-Palette Generation* and *C³-Palette Assignment*) generally support the fundamental visual separability of the classes. It is worth noting that the error rate of the *C³-Palette Generation* is comparable to *Palettailor* which is the start-of-the-art palette generation method for visual discriminability, while the *C³-Palette Assignment* is comparable to the *Optimized Assignment* which is the start-of-the-art palette assignment method for visual discriminability. This indicates that our approach maintains the class discriminability of the scatterplot while enhances the class saliency to help user observe changes between different scatterplots.

It is obvious that the *Alpha Blending* has a much higher error rate than other methods for the discrimination task. As one of the participants said, “The ones that were harder were ones that had colors that when they overlapped would change color. It made it hard to tell if it was the same color or if it was a new color. When the colors were uniform and all the same opacity, it was much easier.” The *Alpha Blending* condition changes the opacity of unchanged classes to make them less attractive, but this will generate new color from color blending, so as to make it hard to distinct them.

Some limitations exist in our evaluation.

First, our experiment mainly focuses on error rate and time consumption, while other measurements were not explored, such as click order of the changed classes and time consumption for each click while *cluster type* might influence the user’s perception. Second, our experiment focuses on identifying the differences between two bar charts or scatterplots, which is a simplified situation, since in real-world cases often more than two visualizations are compared. Third, we cannot further analyze the effect of the *change type*, given the current study design, though we did observe that our methods are more effective for certain types of change.

That brings us to a series of more fundamental questions: how can we properly define the types of changes? What is the just noticeable change magnitude for each change type? Further research is needed to answer these questions so that our approach can be thoroughly evaluated.

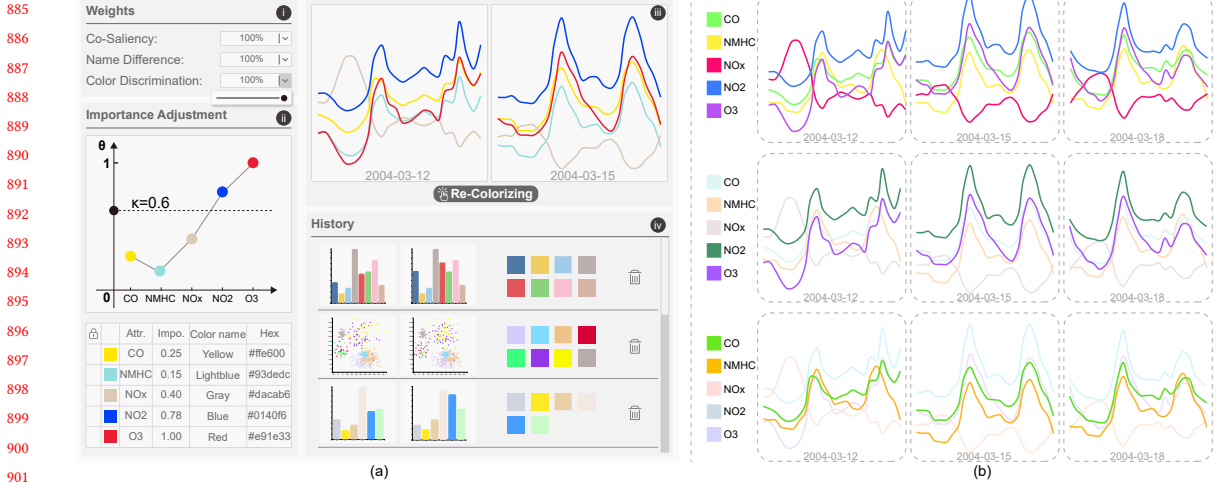


Fig. 7. Our interactive colorization system and a case study. (a) Screenshot of the system consisting of four panels: (i) control panel; (ii) importance adjustment panel; (iii) visualization panel; and (iv) history panel. (b) Using the system to explore the changes of gases in an air quality data set [9]: (top) An automatically generated palette creates salient colors for lines; (middle, bottom) the palettes highlighting two lines with small changes generated by our methods without and with colour name constraint.

5 INTERACTIVE SYSTEM

To help users interactively design colors for comparing multi-class scatterplots, we developed a web-based multi-view visualization tool² (see the screenshot in Fig. 7(a)). It consists of four coordinated views: (i) a control panel, (ii) an importance adjustment panel for selecting κ and the importance of each class, (iii) the juxtaposed visualizations, and (iv) a history view.

After uploading multiple labeled datasets, the system automatically finds an optimal color mapping scheme to colorize the input data, while each class is encoded as a dot on the x-axis of the importance adjustment view indicating the change degree. If the user likes the color mapping scheme, s/he can save it to the history view. By default, our system finds a color mapping scheme that highlights classes with large changes and renders them in ascending order of the corresponding change degrees. To facilitate a coherent exploration, we provide a color name constraint for palette generation, so that the consistency of color names will be preserved in the produced palettes.

Color Name Constraints. Adjusting class importance and κ allows to highlight classes of interest with newly generated color palettes. However, this might not be intuitive for users, since the colors might be completely changed in the new palette. To address this issue, one straightforward way is to assign large opacities to classes of interest and small values to de-emphasized classes. However, this method might not be able to let such classes pop out, since their assigned colors often have a low contrast with the background (e.g., the yellow class in the top of Fig. 7(b)).

To maintain consistent color schemes and highlight classes of interest, we introduce a color name constraint [18] for palette generation. Specifically, the name difference between the new color and the one in the previous palette should be smaller than a threshold during the search for new palettes. In doing so, such selected classes can be easily identified from the new colorization results (see an example in the bottom of Fig. 7(b)).

²<https://c3-palette.github.io/>

937 **5.1 Case Study**

938 To shed further light onto the ecological validity of our approach, we conducted a case study on a real-world categorical
 939 dataset visualized with three line charts. Here, we analyze an air quality data set [9] that contains hourly responses of a
 940 gas multi-sensor device deployed in an Italian city from March 12 to March 18, 2014. The top in Fig. 7(b) shows the
 941 juxtaposed line graphs encoded by our generated color palette, where each gas type is represented by a line with a
 942 unique color. We can see that all gases are encoded with highly salient colors, making it hard to explore changes of
 943 specific gases. This is reasonable because the default κ is zero, but all gases have large changes. Thanks to our interaction
 944 mechanism, users can directly select classes of interest to be highlighted by assigning them a large importance, while
 945 the θ values of the other classes are set to -1. Using the color name constrained palette generation method, the produced
 946 palette lets the selected lines pop out from the others (see the bottom in Fig. 7(b)). Hence, users can easily explore the
 947 changes of the selected two gases (NO_2 and O_3) in the three juxtaposed views.
 948

949

950

951 **6 CONCLUSION AND FUTURE WORK**

952

953 We presented C^3 -palette, a data-aware approach for producing color palettes for comparing horizontally juxtaposed
 954 categorical visualizations that allows a better identification of the biggest change between two data series, while
 955 maintaining the visual discrimination of classes. This goal is achieved by a novel co-saliency model, which characterizes
 956 the most co-salient features between juxtaposed labeled data visualizations while maintaining class discrimination in
 957 the individual visualizations. We evaluated C^3 -palette through a crowd-sourcing study, which empirically demonstrates
 958 that our produced palettes allow for an efficient visual comparison and good class discrimination.

959

960 Our work concentrated on juxtaposed comparisons to detect changes between multiple datasets, whereas its optimal
 961 color palette might not be appropriate for understanding other analytical comparison tasks (e.g., correlation tasks,
 962 rf. [35]). Future work needs to investigate the effectiveness and extensions of our approach for such comparison tasks.
 963 Furthermore, mark shape [28] and mark size [39] might have an effect on the perceptual precision of visual comparisons
 964 and we will explore the possibility to model the influence of these factors.

965

966 Second, our approach produces colors with salient hue to highlight classes with large changes, but those colors
 967 do not visually indicate the ranking of class changes. It would be helpful to associate a color ordering constraint [5]
 968 with the degree of changes, so that the ranking of class changes can be shown clearly. On the other hand, our method
 969 can be extended to generate palettes for people with color vision deficiency by incorporating a physiologically-based
 970 model [32] into our optimization framework.

971

972 Third, while our second user study only examined the interaction effect between change magnitude and different
 973 colorization methods, we plan to investigate how this effect is influenced by different types of changes in scatterplots,
 974 such as point number, center position and shape. The order of rendering is critical for the comparison task and in this
 975 paper we treat it simply by rendering less important classes first. But when there are multiple important large classes at
 976 the same positions, less important classes might be overlapped and hard to distinguish. Thus a professional render
 977 order algorithm would be necessary for multi-class scatterplot rendering.

978

979 Last, our study only evaluated the effectiveness of our palettes with horizontally juxtaposed visualizations, while there
 980 are different layout methods such as vertical arrangement, mirrored arrangement, overlaid, and animation. Previous
 981 studies [35] show that animation performs well in identifying the largest difference and we will conduct studies to learn
 982 how well our palette works in this setting. On the other hand, there are a few different visual comparison methods [14]

983

985

986

987

988

such as plotting differences and faceting groups [45]. It would be helpful to fully investigate the strengths and limitations of each of these methods for visual comparisons.

REFERENCES

- [1] D. Albers, C. Dewey, and M. Gleicher. 2011. Sequence Surveyor: leveraging Overview for Scalable Genomic Alignment Visualization. *IEEE Transactions on Visualization and Computer Graphics* 17, 12 (2011), 2392–2401. <https://doi.org/10.1109/TVCG.2011.232>
- [2] M. Aupetit and M. Sedlmair. 2016. SepMe: 2002 New visual separation measures. In *2016 IEEE Pacific Visualization Symposium*. 1–8. <https://doi.org/10.1109/PACIFICVIS.2016.7465244>
- [3] Patrick Baudisch and Carl Gutwin. 2004. Multiblending: displaying overlapping windows simultaneously without the drawbacks of alpha blending. In *Proceedings of the SIGCHI conference on Human factors in computing systems*. 367–374.
- [4] Ali Borji, Ming-Ming Cheng, Qibin Hou, Huaiyu Jiang, and Jia Li. 2019. Salient object detection: a survey. *Computational Visual Media* 5, 2 (2019), 117–150. <https://doi.org/10.1007/s41095-019-0149-9>
- [5] R. Bujack, T. L. Turton, F. Samsel, C. Ware, D. H. Rogers, and J. Ahrens. 2018. The Good, the Bad, and the Ugly: a Theoretical Framework for the Assessment of Continuous Colormaps. *IEEE Transactions on Visualization and Computer Graphics* 24, 1 (2018), 923–933. <https://doi.org/10.1109/TVCG.2017.2743978>
- [6] H. Chen, W. Chen, H. Mei, Z. Liu, K. Zhou, W. Chen, W. Gu, and K. Ma. 2014. Visual Abstraction and Exploration of Multi-class Scatterplots. *IEEE Transactions on Visualization and Computer Graphics* 20, 12 (2014), 1683–1692. <https://doi.org/10.1109/TVCG.2014.2346594>
- [7] J. Chuang, D. Weiskopf, and Torsten Möller. 2009. Energy Aware Color Sets. *Computer Graphics Forum* 28 (2009). <https://doi.org/10.1111/j.1467-8659.2009.01359.x>
- [8] Charles E. Connor, Howard E. Egeth, and Steven Yantis. 2004. Visual Attention: bottom-Up Versus Top-Down. *Current Biology* 14, 19 (2004), R850–R852. <https://doi.org/10.1016/j.cub.2004.09.041>
- [9] S. De Vito, E. Massera, M. Piga, L. Martinotto, and G. Di Francia. 2008. On field calibration of an electronic nose for benzene estimation in an urban pollution monitoring scenario. *Sensors and Actuators B: Chemical* 129, 2 (2008), 750–757. <https://doi.org/10.1016/j.snb.2007.09.060>
- [10] James T Enns. 1990. Three-dimensional features that pop out in visual search. (1990).
- [11] H. Fu, X. Cao, and Z. Tu. 2013. Cluster-Based Co-Saliency Detection. *IEEE Transactions on Image Processing* 22, 10 (2013), 3766–3778. <https://doi.org/10.1109/TIP.2013.2260166>
- [12] Eiji Fukuba, Hajime Kitagaki, Akihiko Wada, Kouji Uchida, Shinji Hara, Takafumi Hayashi, Kazushige Oda, and Nobue Uchida. 2009. Brain Activation during the Spot the Differences Game. *Magnetic Resonance in Medical Sciences* 8, 1 (2009), 23–32. <https://doi.org/10.2463/mrms.8.23>
- [13] M. Gleicher. 2018. Considerations for Visualizing Comparison. *IEEE Transactions on Visualization and Computer Graphics* 24, 1 (2018), 413–423. <https://doi.org/10.1109/TVCG.2017.2744199>
- [14] Michael Gleicher, Danielle Albers, Rick Walker, Ilir Jusufi, Charles D. Hansen, and Jonathan C. Roberts. 2011. Visual Comparison for Information Visualization. *Information Visualization* 10, 4 (2011), 289–309. <https://doi.org/10.1177/1473871611416549>
- [15] C. C. Gramazio, D. H. Laidlaw, and K. B. Schloss. 2017. Colorgorical: creating discriminable and preferable color palettes for information visualization. *IEEE Transactions on Visualization and Computer Graphics* 23, 1 (2017), 521–530. <https://doi.org/10.1109/TVCG.2016.2598918>
- [16] Mark Harrower and Cynthia A. Brewer. 2003. ColorBrewer.org: an online tool for selecting colour schemes for maps. *The Cartographic Journal* 40, 1 (2003), 27–37. <https://doi.org/10.1179/000870403235002042>
- [17] Christopher G Healey, Kellogg S Booth, and James T Enns. 1995. Visualizing real-time multivariate data using preattentive processing. *ACM Transactions on Modeling and Computer Simulation* 5, 3 (1995), 190–221. <https://doi.org/10.1145/217853.217855>
- [18] Jeffrey Heer and Maureen Stone. 2012. Color naming models for color selection, image editing and palette design. 1007–1016. <https://doi.org/10.1145/2207676.2208547>
- [19] L. Itti, C. Koch, and E. Niebur. 1998. A model of saliency-based visual attention for rapid scene analysis. *IEEE Transactions on Pattern Analysis and Machine Intelligence* 20, 11 (1998), 1254–1259. <https://doi.org/10.1109/34.730558>
- [20] David E. Jacobs, Dan B. Goldman, and Eli Shechtman. 2010. Cosaliency: where People Look When Comparing Images. In *Proceedings of the 23nd Annual ACM Symposium on User Interface Software and Technology*. 219–228. <https://doi.org/10.1145/1866029.1866066>
- [21] H. Jänicke and M. Chen. 2010. A Salience-based Quality Metric for Visualization. *Computer Graphics Forum* 29, 3 (2010), 1183–1192. <https://doi.org/10.1111/j.1467-8659.2009.01667.x>
- [22] N. Jardine, B. D. Ondov, N. Elmqvist, and S. Franconeri. 2020. The Perceptual Proxies of Visual Comparison. *IEEE Transactions on Visualization and Computer Graphics* 26, 1 (2020), 1012–1021. <https://doi.org/10.1109/TVCG.2019.2934786>
- [23] Hye-Rin Kim, Min-Joon Yoo, Henry Kang, and In-Kwon Lee. 2014. Perceptually-Based Color Assignment. *Computer Graphics Forum* 33, 7 (2014), 309–318. <https://doi.org/10.1111/cgf.12499>
- [24] Y. Kim and A. Varshney. 2006. Saliency-guided Enhancement for Volume Visualization. *IEEE Transactions on Visualization and Computer Graphics* 12, 5 (2006), 925–932. <https://doi.org/10.1109/TVCG.2006.174>
- [25] Harold W Kuhn. 1955. The Hungarian method for the assignment problem. *Naval Research Logistics Quarterly* 2, 1-2 (1955), 83–97. https://doi.org/10.1007/978-3-540-68279-0_2

- 1041 [26] S. Lee, M. Sips, and H. Seidel. 2013. Perceptually Driven Visibility Optimization for Categorical Data Visualization. *IEEE Transactions on Visualization and Computer Graphics* 19, 10 (2013), 1746–1757. <https://doi.org/10.1109/TVCG.2012.315>
- 1042 [27] Sharon Lin, Julie Fortuna, Chinmay Kulkarni, Maureen Stone, and Jeffrey Heer. 2013. Selecting Semantically-Resonant Colors for Data Visualization. *Computer Graphics Forum* 32, 3 (2013), 401–410. <https://doi.org/10.1111/cgf.12127>
- 1043 [28] Tingting Liu, Xiaotong Li, Chen Bao, Michael Correll, Changehe Tu, Oliver Deussen, and Yunhai Wang. 2021. Data-Driven Mark Orientation for Trend Estimation in Scatterplots. In *Proceedings of the 2021 CHI Conference on Human Factors in Computing Systems*. 1–16.
- 1044 [29] María-Jesús Lobo, Emmanuel Pietriga, and Caroline Appert. 2015. An Evaluation of Interactive Map Comparison Techniques. In *Proceedings of the 33rd Annual ACM Conference on Human Factors in Computing Systems*. 3573–3582. <https://doi.org/10.1145/2702123.2702130>
- 1045 [30] K. Lu, M. Feng, X. Chen, M. Sedlmair, O. Deussen, D. Lischinski, Z. Cheng, and Y. Wang. 2021. Palettailor: discriminable colorization for categorical data. *IEEE Transactions on Visualization and Computer Graphics* 27, 2 (2021), 475–484. <https://doi.org/10.1109/TVCG.2020.3030406>
- 1046 [31] S. LYi, J. Jo, and J. Seo. 2021. Comparative Layouts Revisited: design Space, Guidelines, and Future Directions. *IEEE Transactions on Visualization and Computer Graphics* 27, 2 (2021), 1525–1535. <https://doi.org/10.1109/TVCG.2020.3030419>
- 1047 [32] G. M. Machado, M. M. Oliveira, and L. A. F. Fernandes. 2009. A Physiologically-based Model for Simulation of Color Vision Deficiency. *IEEE Transactions on Visualization and Computer Graphics* 15, 6 (2009), 1291–1298. <https://doi.org/10.1109/TVCG.2009.113>
- 1048 [33] L. E. Matzen, M. J. Haass, K. M. Divis, Z. Wang, and A. T. Wilson. 2018. Data Visualization Saliency Model: A Tool for Evaluating Abstract Data Visualizations. *IEEE Transactions on Visualization and Computer Graphics* 24, 1 (2018), 563–573. <https://doi.org/10.1109/TVCG.2017.2743939>
- 1049 [34] Tamara Munzner, François Guimbretière, Serdar Tasiran, Li Zhang, and Yunhong Zhou. 2003. TreeJuxtaposer: scalable Tree Comparison Using Focus+Context with Guaranteed Visibility. *ACM Transactions on Graphics* 22, 3 (2003), 453–462. <https://doi.org/10.1145/882262.882291>
- 1050 [35] B. Ondov, N. Jardine, N. Elmquist, and S. Franconeri. 2019. Face to face: evaluating visual comparison. *IEEE Transactions on Visualization and Computer Graphics* 25, 1 (2019), 861–871. <https://doi.org/10.1109/TVCG.2018.2864884>
- 1051 [36] Zening Qian and Jessica Hullman. 2017. Keeping multiple views consistent: constraints, validations, and exceptions in visualization authoring. *IEEE Transactions on Visualization and Computer Graphics* 24, 1 (2017), 468–477. <https://doi.org/10.1109/TVCG.2017.2744198>
- 1052 [37] Yossi Rubner, Carlo Tomasi, and Leonidas J. Guibas. 2000. The Earth Mover's Distance as a Metric for Image Retrieval. *International Journal of Computer Vision* 40, 2 (2000), 99–121. <https://doi.org/10.1023/A:1026543900054>
- 1053 [38] V. Setlur and M. C. Stone. 2016. A Linguistic Approach to Categorical Color Assignment for Data Visualization. *IEEE Transactions on Visualization and Computer Graphics* 22, 1 (2016), 698–707. <https://doi.org/10.1109/TVCG.2015.2467471>
- 1054 [39] Stephen Smart and Danielle Albers Szafir. 2019. Measuring the separability of shape, size, and color in scatterplots. In *Proceedings of the 2019 CHI Conference on Human Factors in Computing Systems*. 1–14.
- 1055 [40] Tableau Software. [n.d.]. The tableau visualization system. <http://www.tableausoftware.com/>.
- 1056 [41] C. Tominski, C. Forsell, and J. Johansson. 2012. Interaction Support for Visual Comparison Inspired by Natural Behavior. *IEEE Transactions on Visualization and Computer Graphics* 18, 12 (2012), 2719–2728. <https://doi.org/10.1109/TVCG.2012.237>
- 1057 [42] C. Tominski, G. Fuchs, and H. Schumann. 2008. Task-driven color coding. In *Proceedings of 12th International Conference Information Visualisation*. 373–380. <https://doi.org/10.1109/IV.2008.24>
- 1058 [43] Yunhai Wang, Xin Chen, Tong Ge, Chen Bao, Michael Sedlmair, Chi-Wing Fu, Oliver Deussen, and Baoquan Chen. 2019. Optimizing color assignment for perception of class separability in multiclass scatterplots. *IEEE Transactions on Visualization and Computer Graphics* 25, 1 (2019), 820–829. <https://doi.org/10.1109/TVCG.2018.2864912>
- 1059 [44] Michelle Q. Wang Baldonado, Allison Woodruff, and Allan Kuchinsky. 2000. Guidelines for Using Multiple Views in Information Visualization. In *Proceedings of the Working Conference on Advanced Visual Interfaces*. 110–119. <https://doi.org/10.1145/345513.345271>
- 1060 [45] Hadley Wickham et al. 2009. Elegant graphics for data analysis. *Media* 35, 211 (2009), 10–1007.
- 1061 [46] Dingwen Zhang, Huazhu Fu, Junwei Han, Ali Borji, and Xuelong Li. 2018. A review of co-saliency detection algorithms: fundamentals, applications, and challenges. *ACM Transactions on Intelligent Systems and Technology* 9, 4 (2018), 1–31. <https://doi.org/10.1145/3158674>
- 1062 [47] L. Zhou and C. D. Hansen. 2016. A Survey of Colormaps in Visualization. *IEEE Transactions on Visualization and Computer Graphics* 22, 8 (2016), 2051–2069. <https://doi.org/10.1109/TVCG.2015.2489649>
- 1063
1064
1065
1066
1067
1068
1069
1070
1071
1072
1073
1074
1075
1076
1077
1078
1079
1080
1081
1082
1083
1084
1085
1086
1087
1088
1089
1090
1091
1092